Estimation of wind energy potential through experimental investigation of boundary layer in small wind tunnel

Cássia S. A. Maia [1], Felipe P. Mariano[1], Andreia A. Nascimento[2], Marlipe G. Fagundes Neto [2]

[1]*Escola de Engenharia Civil e Ambiental, Universidade Federal de Goiás*
Av. Universitária, 1488, Setor Leste Universitário, CEP 74690-900, Goiás, Goiânia, Brasil
csacassia@gmail.com
[2]*Escola de Engenharia Elétrica, Mecânica e de Computação, Universidade Federal de Goiás*
Av. Esperança, s/n, Campus Samambaia, Al. Ingá, B5, CEP: 74.690-900, Goiás, Goiânia, Brasil
fpmariano@ufg.br, aanascimento@ufg.br, marlipe@ufg.br

Abstract. The first step in harnessing wind energy is to assess the wind potential of the site where a turbine or wind farm is to be installed. This involves predicting the potential for generating electrical power from the kinetic energy of the wind. Furthermore, understanding the local wind regime is a crucial parameter in determining the necessary characteristics of the wind turbines to be installed in that area. This paper presents a literature review on experimental techniques for generating boundary layers in wind tunnels. Additionally, this work pertains to an experimental study conducted in the wind tunnel provided by Eletrobras/FURNAS, focusing on the variation of the boundary layer using an apparatus known as the boundary layer flat plate, which contains installed pressure probes and a flap mechanism at the trailing edge. The objective of these experiments is to develop a control model for boundary layer height to estimate wind potential. Different combinations of angles (-10°, +10°, 0°, -20°, +20°) and velocities (6, 13, 20, 26, and 33 m/s) were tested. The results indicate that modifying the flap angle significantly alters the boundary layer generated over the plate. Analyzing the angle independently of each velocity shows that the boundary layer generated is significantly different for all the studied velocities.

Keywords: wind energy; flow over flat plate; boundary layer, wind tunnel.

1 Introduction

In Brazil, the consumption of electrical energy has shown continuous growth, mainly due to economic and technological development in recent years, Breitenbach [1]. The increasing industrialization, population growth, and consequent increase in the use of energy-consuming equipment necessitate a parallel growth in generation, transmission, and distribution, which does not always keep pace with consumption Breitenbach [1]. Additionally, the generation of electrical energy from hydroelectric power is compromised due to climate change. The quickest solution found by the federal government and Brazilian energy management agencies to address this issue has been the use of thermoelectric power plants, which generate electricity through the combustion of fossil fuels, specifically petroleum and coal derivatives, Viola et al. [2].

However, resorting to thermoelectric plants, aside from other disadvantages, increases the greenhouse effect (Viola et al. [2]), resulting in global temperature rise, which further exacerbates climate change, such as reduced rainfall and extreme heat waves, Coimbra and Tibúrcio [3]. Thus, in the face of the need for electrical energy, there is a cycle of environmental heating and destruction. Therefore, it is crucial to invest in alternative forms of obtaining electrical energy, specifically. In this context, one option is wind energy, derived from the wind, which is considered a clean and renewable energy source.

Studies on wind energy encompass turbine design to wind potential analysis in the areas of interest.

Investments are still necessary to improve research in areas such as turbine efficiency and wind potential. It is important to note that the first step in harnessing wind energy is to assess the wind potential of the site where a turbine or wind farm is to be installed. Understanding the wind potential of an area directly influences company decisions, as the correct acquisition of land and specific wind turbines for a given local wind regime produces high-quality electrical energy, increasing continuity indices.

Tests to obtain wind potential can be conducted in the field or using Fluid Dynamics, which can be analytical, numerical-computational, or experimental. Conan [4] adds that field measurements are limited to sparse locations that may not reflect the conditions of the entire site. This is particularly true in complex terrains. Therefore, on the scale of a large wind farm, other tools are needed.

Studies in the experimental area include experiments conducted in atmospheric boundary layer wind tunnels. Wind tunnels can be defined as experimental equipment that uses the principle of relative motion between the fluid and the tested model. Furthermore, they are designed to develop an artificial flow that models the free stream, which should have a constant velocity over time and throughout the cross-section area of the test section inlet, Cardoso [5]. They are divided into two categories, open or closed circuit. Open circuit systems do not recirculate air and are more economically viable. They consist of three main structures: a nozzle, a test section, and a diffuser. In a closed-circuit tunnel, the air recirculates within the system, thus it has more components and is a more complex and costly system, Queiroga [6].

The velocity distribution along the inlet section and over time is one of the most important parameters for flow quality to ensure reliable experimental results, Cardoso [5]. However, to achieve good results, it is important to correctly simulate the atmospheric boundary layer (ABL) in wind tunnels. The boundary layer (BL) is a thin region adjacent to the surface where the flow is retarded by the influence of friction between the solid and the fluid. This small layer has a strong influence on drag and heat transfer to the body.

Several studies have already been conducted demonstrating the several techniques used to simulate the development and control of the ABL over different types of terrains with wind tunnels of different sizes and models, necessitating continuous study given the importance of the subject. Thus, in the present work, it is proposed to use the experimental apparatus called the "boundary layer plate," which consists of a flat plate with differentiated roughness and a mechanism similar to an aerodynamic flap positioned at its trailing edge. When actuated, this mechanism modifies the height of the boundary layer produced over the plate. Using factorial design, ANOVA, and other statistical tools, it is determined which flap angles significantly alter the boundary layer height within the wind tunnel test section.

2 Methodology

In the present work, an open-circuit, subsonic wind tunnel provided by Eletrobras/FURNAS is used, which has a test section with a cross-sectional area of 0.46 m x 0.46 m and a length of 1.1 m, capable of reaching speeds up to 35 m/s. The experimental apparatus called the boundary layer flat plate is inserted into the test section, as shown in Figure 1 (left).

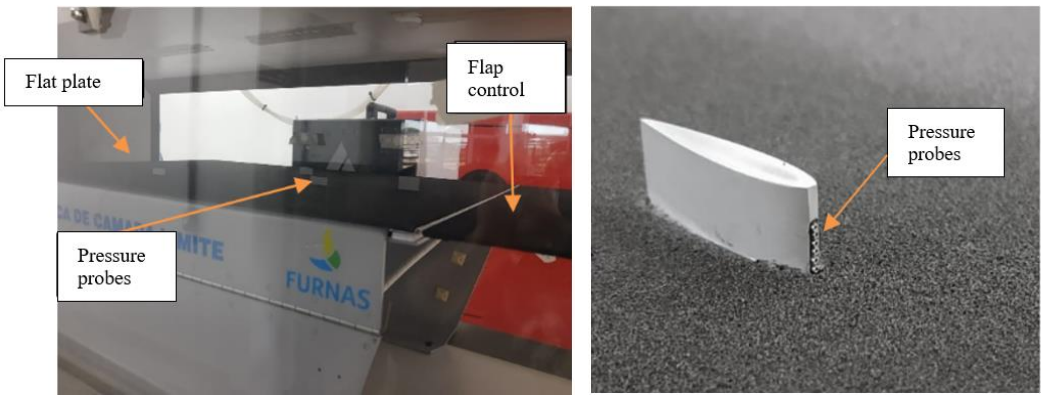

Figure 1. Flat plate for boundary layer development study: positioned inside the test section of the wind tunnel (left), detail of pressure sensors (right).

This plate is equipped with total pressure (P_{total}) measurement sensors distributed along its length (Fig. 1 right), and at the trailing edge, there is a flap mechanism (Fig. 1 left), which allows for altering the effective flow angle over the plate. Additionally, a Pitot tube is used, with the total pressure port closed and the static pressure port (P_e) open, positioned above the pressure sensors. The outputs and connections of these two tubes are directly connected to a digital pressure module. Thus, the difference between total pressure and static pressure is obtained at several points in the wind tunnel test section. Using these values, applying Bernoulli's equation eq. (1) along a streamline reaching a sensor:

$$\frac{P_{\text{total}}}{\rho g} = \frac{P_e}{\rho g} + \frac{V^2}{2g}, \tag{1}$$

where g is gravity, taken as 9.81 m/s^2, ρ is the air density in kg/m^3, obtained from the temperature and humidity readings from sensors inside the wind tunnel, and V is the average flow velocity in m/s. By rearranging eq. (1), the flow velocity at a sensor on the flat plate is given by:

$$V = \sqrt{\frac{2(P_{\text{total}} - P_e)}{\rho}}. \tag{2}$$

The experimental procedure involves obtaining the total pressure from each sensor and the static pressure from the Pitot tube for different flow velocities (m/s) and different flap angles (°). The velocities are manually adjusted by setting the motor's rotational speed using the wind tunnel's frequency inverter. The experiment is conducted for combinations of flap angles and rotational velocity (-20°, -10°, 0°, +10°, +20° and 6, 13, 20, 26, and 33 m/s), resulting in 25 experimental configurations.

The following steps outline the experimental procedure. First, the flap is set to a specific angle of attack, and the wind tunnel is started at a specified velocity. After waiting at least 30 s to ensure the flow becomes statistically steady, the pressure acquisition mode is activated to measure the pressure at a sampling rate of 3.0 Hz for at least 60 s. The wind tunnel is then turned off, a new flap angle and velocity are set, and the experiment is repeated.

Temperature and humidity measurements were taken for each pressure reading in the wind tunnel, resulting in a table of total and static pressure data over the 60 s acquisition period, yielding 180 data points from the pressure sensors. The study presents data from 8 sensors aligned vertically near the trailing edge of the flat plate. It is important to note that four replicas were performed, and the experiment order was randomized, as recommended by Montgomery [7].

3 Results

As results, the mean total and static pressures obtained over the acquisition time are calculated. Then, the mean pressure results in eq. (2) are used, converting them into mean velocity (over time) at a specific point of the flow over the flat plate. This calculation is performed for the 25 measurements (combination of 5 angles and 5 velocities) at different 8 positions along the vertical.

Thus, the results are grouped into graphs in Figure 2, where curves of mean velocity (over time) along different vertical positions (y) of the sensors are presented. To describe and differentiate the curves in the graphs, the letters "A" and "V" are used to represent angle and velocity, respectively.

It is possible to observe that, for positive flap angles (+10º and +20º), the boundary layer height becomes defined at lower velocity, allowing for a direct estimation of its height. However, for negative flap angles (-20º and -10º) and for the zero angle (0°), the boundary layer is still developing, as the profile of mean velocity has not yet stabilized at a specific velocity.

Another important result is the variation in velocity: the boundary layer is better defined at lower velocities. At higher velocities, even with a higher positive flap angle (+20º), the boundary layer cannot be determined with the available sensors for the average velocity of 33 m/s.

3.1 Statistical analyses

Statistical analyses were conducted using the Minitab19 statistical software in its DEMO version. Firstly, an

Analysis of Variance (ANOVA) was performed on the imposed velocity to verify if the combination of angle and velocity significantly influenced the formation of the boundary layer height. Subsequently, the same procedure was separately performed for each velocity, *i.e.*, a one-way ANOVA for the variation in flap angle.

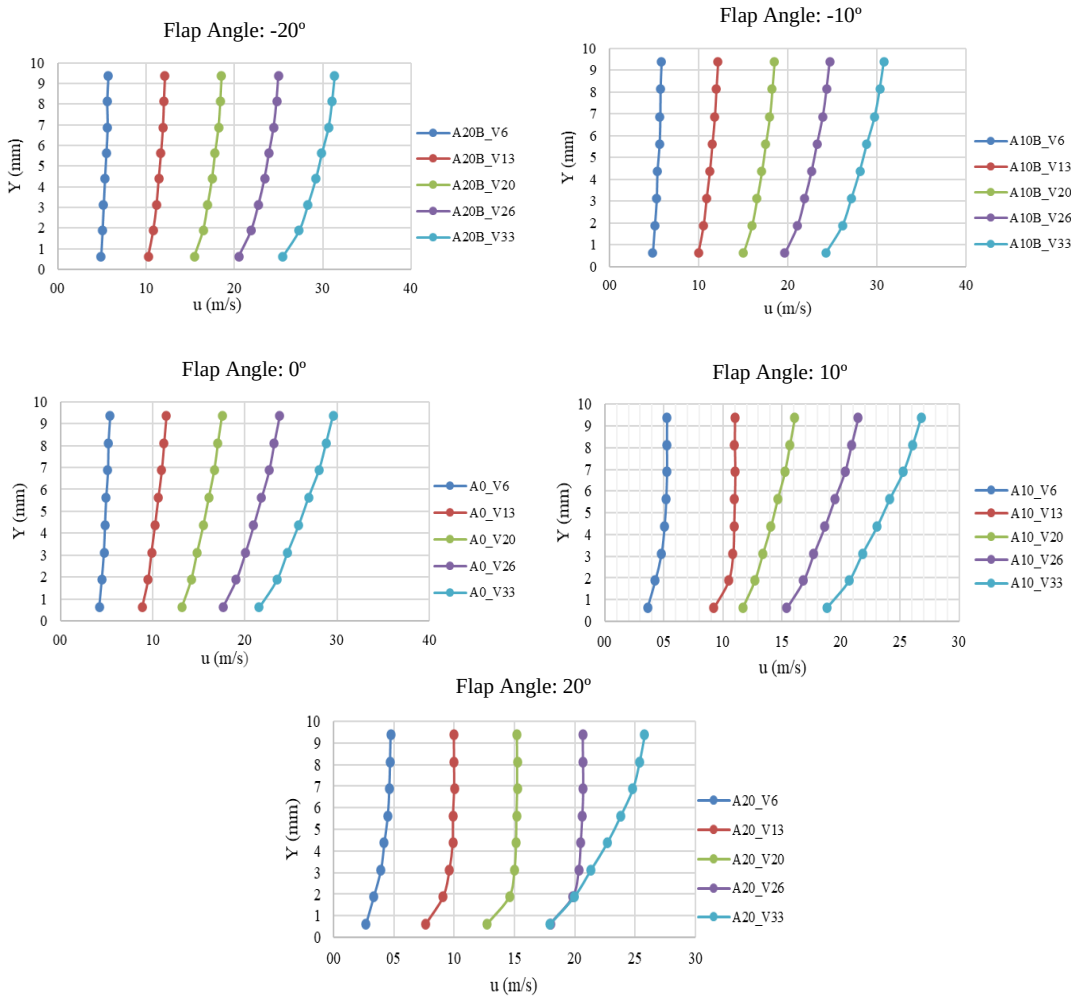

Figure 2. Distributions of mean velocity along the pressure acquisition sensors, for different flap angles.

As the response surface, the boundary layer height (δ) was used, which is the height from the flat plate surface where the flow velocity becomes 99% of the inlet flow velocity, for each combination obtained from the mean of the collected data. In cases where stabilization did not occur, a height greater than 10 mm was considered, taking into account that the last sensor reading point is 9.375 mm from the floor of the flat plate.

3.2 ANOVA with 2 Factors: Angle and Velocity

The Analysis of Variance (Tab. 1) shows that the contribution of flap angle variation is 15.50%, velocity variation is 44.53%, and their interaction contributes 32.52%. Based on these results, the null hypothesis can be rejected (p-value is less than the significance level of 0.05), concluding that the boundary layer undergoes significant variation with changes in flap angle and velocity within the wind tunnel.

Table 1. Analysis of Variance.

Fonte	GL	SQ Seq	Contribution	SQ (Aj.)	QM (Aj.)	Valor F	Valor-P
Model	27	713.672	92.59%	713.672	26.4343	33.32	0.000
Blocking (replicates)	3	0.297	0.04%	0.297	0.0990	0.12	0.945
Linear	8	462.688	60.03%	462.688	57.8359	72.90	0.000
Angle	4	119.469	15.50%	119.469	29.8672	37.64	0.000
Velocity	4	343.219	44.53%	343.219	85.8047	108.15	0.000
Angle*Velocity	16	250.688	32.52%	250.688	15.6680	19.75	0.000
Error	**72**	**57.125**	**7.41%**	57.125	0.7934		
Total	**99**	**770.797**	**100.00%**				

The summary in Tab. 2, which shows the model summary values, indicates that the coefficient of determination (R^2) is 92.59%, confirming the model fit.

Table 2. Model Summary.

S	R^2	R^2 (aj)	PRESQ	R2 (pred)
0.890732	92.59%	89.81%	110.195	85,70%

By analyzing Figure 3, which presents the residual and fit plots, it is observed that the residuals follow a normal distribution with zero mean, which supports the data analysis by ANOVA. In the residual versus order plot, the assumption is that the residuals show no trends or patterns when displayed in temporal order. Finally, the model containing the main factors and their interaction is adequate and satisfies the assumptions of the analysis.

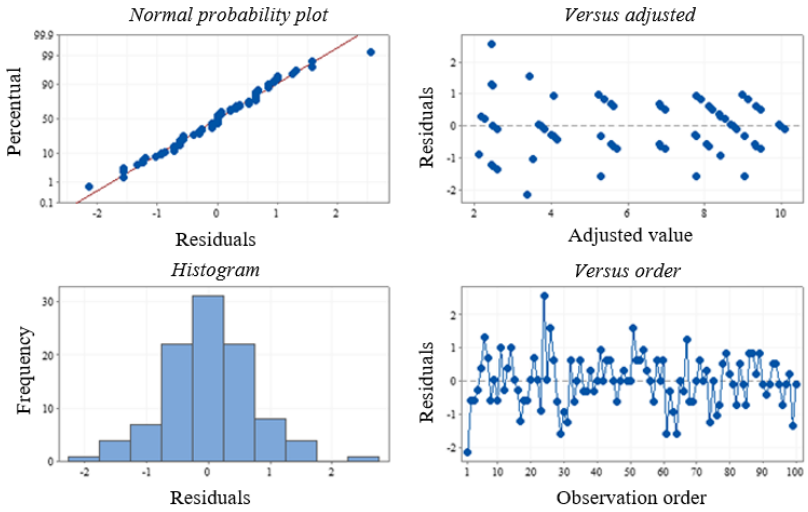

Figure 3. Results presented in Residual vs. Imposed Velocity response plots.

3.3 One-Way ANOVA: Angle

In Tab. 3 are presented the key values for all velocities.

Table 3. Key values for the studied velocities.

Velocity	6.0 m/s	13 m/s	20 m/s	26 m/s	33 m/s
P-value	0,01	0,00	0,00	0,00	0,00

Contribution Angle	56,63%	91,16%	94,82%	86,61%	73,28%
R^2 fit	45,06%	88,81%	93,43%	83,04%	66,16%

Observing Table 3, the null hypothesis can be rejected (P-value is less than the significance level of 0.05) for all studied velocities. Therefore, it is concluded that the boundary layer undergoes significant variation with changes in the flap angle at velocities ranging from 6.0 m/s to 33 m/s in the wind tunnel.

3.4 Metamodel Determination

The determination of the best model was performed by combining several variables using the Minitab19 program in its DEMO version, aiming for a regression equation with an appropriate adjusted R^2 when evaluated alongside other statistical variables, then a simpler regression equation, eq. (3), and another with more variable combinations, eq. (4), were chosen:

$$\delta = 15.63 + 2.621V - 0.243A - 0.0717AA \tag{3}$$

$$\delta = -22.4 + 6.99V + 2.051A - 0.1003VV + 0.1618AA - 0.3160VA \ldots \\ \ldots + 0.00823VVA - 0.02763VAA + 0.000650VVAA \tag{4}$$

The correlation coefficient (R^2) of Model 2 (Tab. 4) is more satisfactory and the R^2(aj) is higher, takes into account the degree of freedom in the fitting model (regression equation), confirming the model fit is better. However, other variables must be analyzed, such as the Variance Inflation Factor (VIF). Ideally, the VIF should be equal to 1.0, indicating more statistical significance for the experiment, showing that the predictors are not correlated.

Table 4. Key statistical values for the metamodels presented in eqs. (1) and (2).

Model	**R^2**	**R^2(aj)**	**VIF**
1	66,41%	65,36%	1.0
2	80,98%	79,31%	19,32 a 160,51

For better understanding, the main results of the metamodels are presented in Figs. 4, *i.e.*, contour plots of boundary layer height ($\delta = Y$) obtain from eqs. (3) and (4), respectively.

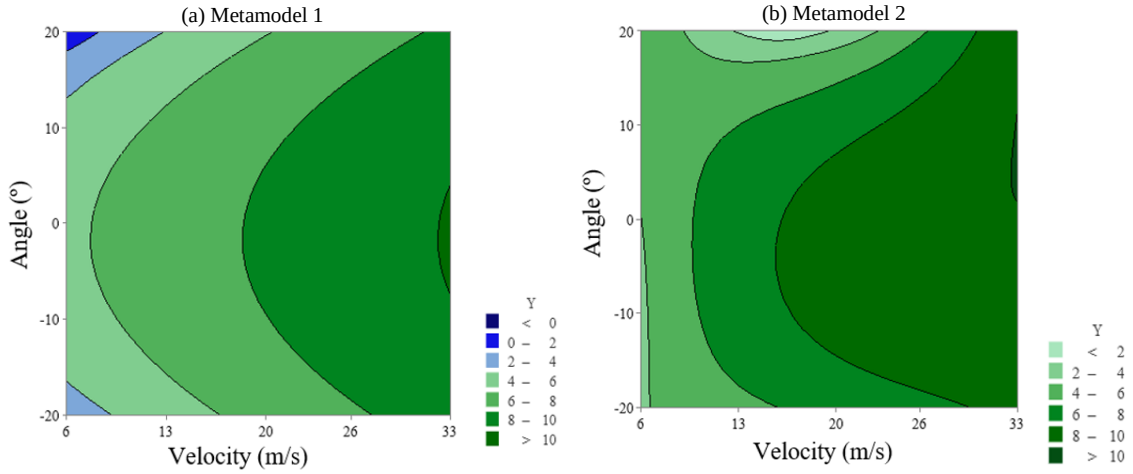

Figure 4. Contour plots of boundary layer height ($\delta = Y$) obtain by metamodels (1) and (2).

Physically, from the plot in Fig. 4(a), it is understood that to simulate a boundary layer height of

approximately $\delta \approx 7.0$ mm, the wind tunnel velocity should be adjusted between 13 m/s < V < 20 m/s, and the flap angle of the flat plate should be around A = 0º. For the same δ, it is possible to increase the speed to 26 m/s by adjusting the flap angle to 15º, thus defining the boundary layer height limits and velocities that the available wind tunnel can simulate.

4 CONCLUSIONS

The present work addressed a method to control a boundary layer height in wind tunnels. As an application, the method of changing the flap angle was used to verify if it is possible to alter the boundary layer height in the wind tunnel. The main result of the adopted method shows the interaction between the flap angle and the boundary layer formation, with a noticeable decrease in boundary layer height for positive angles and an increase for negative angles. Furthermore, it is observed that higher velocities result in a higher boundary layer, as expected for more turbulent flows.

In applying the present study in practice, an adjustment of the current model was proposed. Thus, the study provided a simpler and a more comprehensive metamodel. Both demonstrated satisfactory results and can be used to determine the boundary layer height for other combinations different from those studied here. Using the experimental setup "flat plate with flap," it is possible to simulate boundary layers of different heights at various velocity ranges, which is fundamental for wind potential studies.

Finally, further developments are planned to demonstrate the influence of the flap angle for other positions along the plate's length and to create a mechanism for automatic flap angle adjustment. This will allow direct control of the boundary layer height, more closely representing wind effects.

Acknowledgements. The authors thank Eletrobras/FURNAS and the Research and Technological Development Program (P&D) of ANEEL for the infrastructure and financial support provided for this work.

Authorship statement. The authors hereby confirm that they are the sole liable persons responsible for the authorship of this work, and that all material that has been herein included as part of the present paper is either the property (and authorship) of the authors or has the permission of the owners to be included here.

References

[1] G. Breitenbach, “Análise do Potencial Eólico para a Geração de Energia Elétrica em São Francisco de Paula, RS, Utilizando Método Computacional WASP”. *Trabalho de Conclusão de Curso*, Centro Universitário Univates, Lajeado, 2016.
[2] M. R. Viola, and C. R. de MELLO and S. C. Chou and S. N. Ynagi and J. L. Gomes, “Assessing climate change impacts on upper Rio Grande basin hydrology, Southeast Brazil”. *Internacional Journal of Climatology*, vol. 35, n. 6, pp. 1054-1068, 2015.
[3] P. Coimbra and J. Tibúrcio, “Geografia: uma Análise do Espaço Geográfico”. Ed. 3, Harbra, 2006.
[4] B. Conan and A. Chaudhari and S. Aubrun and J. van Beeck and J. Hämäläinen and A. Hellsten “Experimental and Numerical Modelling of Flow over Complex Terrain: The Bolund Hill”. *Boundary-Layer Meteorol*ogy, vol. 208, pp. 158-183, 2016.
[5] F. R. M. Cardoso, “Caracterização experimental de túneis de vento para a análise de potencial eólico”. *Dissertação de Mestrado em Engenharia Ambiental e Sanitária*, Universidade Federal de Goiás, Goiânia, 2020.
[6] A. L. Queiroga, “Projeto de Túnel de Vento”. *Trabalho de Conclusão de Curso em Engenharia Aeroespacial*. Universidade de Brasília, Gama, 2022.
[7] D. C. Montgomery “Design and Analysis of Experiments”. Ed. 8, John Wiley & Sons, Inc., 2013.